

# Evaluation of TOPSAR DEMs for geomorphic studies of landform modification, Long Valley caldera area, Nevada-California

Donald M. Hooper<sup>1</sup>      Marcus I. Bursik<sup>2</sup>      Frank H. Webb<sup>3</sup>

February 10, 2002

<sup>1</sup>Center for Earth and Environmental Science  
State University of New York at Plattsburgh  
Plattsburgh, NY 12901 U.S.A.

<sup>2</sup>Department of Geology  
State University of New York at Buffalo  
Buffalo, N.Y. 14260 U.S.A.  
mib@geology.buffalo.edu (corresponding author)

<sup>3</sup>Propulsion Laboratory  
California Institute of Technology  
Pasadena, CA 91109 U.S.A.

In October 1996 the airborne TOPSAR instrument was flown over the Long Valley caldera region, California-Nevada. Topography calculated from TOPSAR data are in the form of a high resolution ( $5 \times 5$  m ground spacing) digital elevation model (DEM). Within this DEM, large, steep fault scarps cut alluvium and alluvial fans in Fish Lake Valley, southeast of Long Valley caldera. The large scarps are the product of multiple offsets rather than a single episode. Other relevant geomorphic features present in the digital topography include splays along the main fault, levees, displaced alluvial fan surfaces, shutteridges, offset drainage, and small normal faults with only 1 - 6 m of offset. Division of the fault zone into sections is possible based on the TOPSAR topography, and is consistent with segmentation suggested by previous workers. Field work corroborated landform character, confirmed fault-scarp morphometry, and aided the evaluation of the accuracy of and potential problems within the DEM.

# 1 INTRODUCTION

By using digital topography derived from TOPSAR, we are able to conduct terrain and geomorphologic analyses of Quaternary fault scarps. Our efforts focus on the large, steep fault scarps found in Fish Lake Valley along the Nevada-California border (Fig. 1). The Fish Lake Valley fault zone (FLVFZ) trends in a northwest-southeast direction for approximately 80 km. It is the northernmost component of the Furnace Creek-Death Valley fault system (e.g., Brogan et al., 1991; dePolo et al., 1993; Reheis and Dixon, 1996; Reheis and Sawyer, 1997). Fish Lake Valley is bounded on the west by the White Mountains and on the east by the Silver Peak Range. To the south, the White Mountains are separated from the Inyo Mountains by Deep Springs Valley. The northern portion of the valley is approximately 25 km wide, but the width decreases to less than 10 km in the southern portion. The eastern White Mountains consist largely of Mesozoic granitic rocks and Cambrian-Precambrian metasedimentary rocks. Late Tertiary volcanic rocks, including those in the Silver Peak Range and Volcanic Hills, locally overlay these older rocks (e.g., Reheis and Sawyer, 1997). The FLVFZ has a variety of late Quaternary neotectonic features that record a long history of recurrent earthquake activity. Geomorphic evidence for fault activity in Fish Lake Valley includes shutterridges, offset drainages, displaced beds of 0.76 Ma Bishop ash, displaced alluvial fans, and large, steep fault scarps that cut alluvium and alluvial fans. The FLVFZ is predominantly characterized by right-lateral strike-slip displacement with locally significant vertical offset. A summary of fault relations shows that displacement on contemporaneous northwest-striking faults is right lateral, on north-striking faults is normal, on northeast-striking faults is left lateral, and on intermediate strikes is oblique (Brogan et al., 1991; Sawyer, 1991; Reheis and Sawyer, 1997).

In this report we focus on normal fault scarps in Fish Lake Valley. These scarps are steep, linear to curvilinear bluffs produced by displacement of the land surface along the fault trace. The initial topographic expression may be degraded as material weathered and eroded from the scarp is deposited as small, fresh alluvial fans and colluvium on the debris slope and wash slope. Because fault movement is often episodic, the height of large scarps is usually the sum of multiple offsets rather than a single episode. Most of the scarps examined in this study have an average height of over 30 m and are therefore produced by multiple tectonic offsets.

## 2 TOPSAR DEM

TOPSAR uses the C-band channel (5.6 cm wavelength) of the JPL/NASA AIRSAR DC-8 airborne synthetic aperture radar system (Zebker et al., 1992).

This instrument comprises two radar antennas that are displaced vertically on the aircraft fuselage to form an interferometer. Radar interferometry exploits the small angular difference in viewing geometry between two images to derive the DEM. The theory and application of radar interferometry are discussed in several references, including Zebker and Goldstein (1986), Zebker et al. (1994), and Madsen et al. (1995). The digital topography used in this study was calculated from TOPSAR data and is in the form of a digital elevation model (DEM) with 5-m spacing and 2 m vertical resolution. The TOPSAR system often produces height measurements on a 10-m spatial grid with vertical relative accuracy ranging from 3-5 m, depending upon the relief of the target (e.g., Zebker et al., 1992; Madsen et al., 1995). These raster-formatted data are a digital representation of a land surface in which northing, easting, and elevation values are recorded for each sampled point of the grid or altitude array. Each TOPSAR scene must be referenced to a geodetic grid before absolute elevations and regional slopes can be resolved (Hensley et al., 1994; Zebker et al., 1994). The point spacing and nominal resolution of these data are almost an order of magnitude better than are the standard digital topographic products available to the public from government agencies.

The acquired DEM covers the Long Valley region of the Sierra Nevada of eastern California and the White Mountains along the California-Nevada border. In this report, our area of interest is the eastern-most region of the DEM, which includes the semi-arid region of Fish Lake Valley. However, the southern margin of the FLVFZ was beyond the flight lines incorporated into the topographic mosaic used for this study. Although the ground surface in the valley at elevations below our study area is moist due to irrigation, at the selected study sites the ground surface was dry at the time the radar data were obtained in October, 1996. Boulders and sagebrush community plants are interspersed over a generally sandy surface of crystalline grains that are derived from the adjacent White Mountains.

The accuracy of topographic maps derived from an interferometric radar technique has been discussed by Zebker et al. (1994) and Hensley et al. (1994). These same workers noted that interferometric data may be characterized by missing data, especially in steeper terrains. These gaps in the data are generally caused by foreshortening or shadowing. There are processing and acquisition methods, such as rotation of viewing angle and various interpolation schemes, that help mitigate these effects. Some strips of missing data are present in the Fish Lake Valley portion of the DEM, usually occurring around mountain peaks or steep canyon walls. A limited number of linear and 'bump-like' artifacts have also been found in the DEM. Visual ground inspection showed that these artifacts were not real (Fig. 2).

By using this topographic dataset, we are able to identify fault splays, levees on the alluvial fan surface, a landslide deposit (centered  $\sim 1$  km north of Perry

Aiken Creek—see Fig. 2), gullies incising fault scarp slopes, and possibly some very large boulders (at the vertical resolution limit). Most importantly for this study, we are able to measure in detail fault scarp morphometry, including height, slope angle, and lateral extent. Many of these morphometric features cannot be discerned in standard 30 m/pixel USGS DEMs.

Several large fault scarps were targeted as individual study sites. From north to south these include those at Indian Creek, Perry Aiken Creek, McAfee Creek, and Wildhorse Creek. These are each large scarps in a narrow zone less than 1 km wide along the range front. The DEM used in this study does not include the southern-most portion of Fish Lake Valley.

### 3 DETECTION OF FAULT SCARPS

With the availability of high resolution digital topography from TOPSAR, there are two methods that can be employed to aid detection of fault scarps: shaded relief maps and slope angle maps. The shaded relief maps are essentially low-sun-angle views of a continuous terrain surface, while the slope angle maps specifically measure gradient. The pseudo-three-dimensional surface was shaded to highlight relief and then colored to represent elevation in an intuitive manner (Fig. 2). Slope angles were calculated by using a three by three search window (or array) of TOPSAR elevation points (or cells) to determine the maximum value. These calculations represent the four general directions, north (N)-south (S), east (E)-west (W), NW-SE, and NE-SW. The algorithm used to calculate slope angle is similar to that described by Gao (1994).

We employed this methodology to compare TOPSAR data to previously published maps of surficial deposits and faults in Fish Lake Valley. Specifically, three different geologic maps can be compared to the DEM: Brogan et al. (1991, their Fig. 5) produced a surficial geologic sketch map for the Perry Aiken Creek area, Reheis et al. (1993) published a 1:24,000-scale geologic map of the Davis Mountain quadrangle that includes the scarps in the Indian Creek region, and Reheis and Sawyer (1997, their Fig. 11) made a geologic sketch map that concentrates upon both Perry Aiken and McAfee Creeks. The larger scarps shown in the geologic maps are easily recognized in the TOPSAR data, but smaller scarps and splays can also be recognized. Because of steep channel walls and cutbanks, major creeks as well as many smaller drainage channels are readily defined in the DEM. The length of shadow helps to determine the height of a scarp or channel wall, and slope maps help reveal the extent and location of some smaller scarps and the detail in overall scarp morphology. Although dependent upon imaging geometry, the high spatial and vertical resolution of the TOPSAR data appears to aid the identification of sharp ridges, peaks, and deep valleys.

## 4 FAULT SCARP MORPHOMETRY

Fault scarps formed in unconsolidated alluvium and colluvium are characterized initially by a steep scarp-slope angle (usually at least  $60^\circ$ ) and a sharp scarp crest. The free face, the exposed surface resulting from faulting, is rapidly degraded by gravity-induced movement of material which then accumulates below on a sloping surface at about the angle of repose ( $\sim 35^\circ$ ). Overland flow then produces a gently sloping wedge of debris at the base of the scarp. A degraded scarp is indicated by a decrease in gradient of the midsection, a decrease in curvature of the basal concavity, and the rounding of the scarp crest. Wallace (1977), Bucknam and Anderson (1979), and Nash (1980) offer detailed studies of the degradation of fault scarps with time. There is a regular decrease in midsection slope angle with estimated age for scarps of a given height. However, age control is poor for scarps in Fish Lake Valley.

Fault scarp profiles or cross-sections were extracted from the DEM at each selected study site. Because of the geometrically-corrected raster format of the data, all profiles are east-west topographic sections and therefore are nearly perpendicular to the trend of each fault. Scarp height and the midsection slope angle are the main morphometric parameters or slope attributes that we focus upon in this study. Scarp height is measured by projecting the upper and lower original surfaces to intersect with a projection of the midslope. The vertical separation between the two intersections of these three lines is the scarp height (Peterson, 1985). The midsection slope angle is the mean angle of the midslope segment. Measurements of scarp morphometry are presented in Table 1 and follow the techniques described in Bucknam and Anderson (1979), Nash (1984), and Peterson (1985).

Perry Aiken Creek and Perry Aiken Creek-South had the longest length of fault scarp analyzed; each was examined over a distance of 290 m. The Indian Creek-South section was 180 m in length, the shortest measured segment. Generally, each study site had a measured section that began or ended with a splay or at a creek or similar drainage channel. Profiles were extracted for every DEM line (northing), but usually there was little variation between adjacent lines and therefore a 10 m spacing rather than a 5 m spacing was used when calculating the morphometry at each study site. Scarp segments marked by gullying, which indicates control by overland flow, were not included in Table 1.

Perry Aiken Creek has the greatest average scarp height and the highest average degraded midsection slope angle. Wildhorse Creek has the lowest average degraded midsection slope angle while Indian Creek-South has the lowest average scarp height. The distribution of these data suggests that the relationship between scarp height and midsection slope angle can be approximated by a linear fit. Significantly large values for scarp height support the interpreta-

tion that these bluffs represent the sum of multiple offsets rather than a single episode.

In addition to the measurement of morphological attributes, the resolution of the data is sufficient to reveal fault splays, variations in scarp height along the fault trend, gullies in the debris and wash slopes, and landslide and/or debris flow deposits. Other morphological characteristics can be observed as the DEM also reveals the gentle slopes of the alluvial fan surface(s) in comparison to the steeper slopes of the range front and steep channel walls, cutbanks, and levees associated with the larger creeks.

By using a clinometer in conjunction with a tape measure, compass, and four-foot-long board, detailed field profiles were measured going west to east across selected scarps. Six of these field profiles were made, including one at Indian Creek, one at Perry Aiken Creek-North, two at Perry Aiken Creek, and two at McAfee Creek. The profiles were matched against profiles extracted from the DEM (Fig. 3). The crest, midslope and lower slope regions typically display different, systematic discrepancies between field and TOPSAR elevations. The cause of these discrepancies is unknown, but must arise from some combination of systematic errors in field or TOPSAR elevations. The crest usually shows positive, sometimes large residuals of field (data) minus TOPSAR (model) elevations. A discrepancy can be expected from radar data wherever there is a sharp break in slope as at the crest. The fit for the midslope region is generally poorer and displays negative residuals, but still mostly within the  $\sim 2$  m vertical resolution. Along the lower portion of the fault scarp (the debris slope and wash slope) there is the closest correspondence between field and TOPSAR measurements, although the residuals tend to have the same sign as they do in the midslope. The elevations of the upper alluvial fan surface and the lower fan surface appear to be well-correlated between the sets of data.

## **5 SECTIONS OF THE FISH LAKE VALLEY FAULT ZONE**

Previous studies have divided the FLVFZ into separate regions based upon the differences in fault strike or trend, width of the fault zone, consistency of fault patterns, and apparent timing of the most recent events. Sawyer (1991) divides Fish Lake Valley into four "subzones": Northern, Dyer, Eastern, and Western. His Western subzone parallels the Eastern subzone and forms the relatively subdued front of the White Mountains. It bends or merges into the through-going Eastern subzone. In their study covering the entire Death Valley-Furnace creek fault system, Brogan et al. (1991) prefer the term "section" and note the difficulty in identifying different subdivisions along an entire fault system. They subdivide Fish Lake Valley into a northern Chiatovich Creek section, a

central Dyer section, and a southern Oasis section. Reheis and Sawyer (1997) subdivide Fish Lake Valley into Chiatovich Creek and Dyer sections identical to those of Brogan et al. (1991). The Dyer section ranges from Busher Creek in the north to Toler Creek in the south. Their study uses a longer Oasis section that includes the Horse Thief Canyon section of Brogan et al. (1991).

The DEM used in this study allows for an examination of the Chiatovich Creek, Dyer, and northern portion of the Oasis sections. Each of these three sections has a regression line with a similar slope (Table 2; Fig. 4). Therefore, both scarp height and midsection slope angle were examined to determine if the populations came from different sections. Results from t-tests with a 10% level of significance (5% in each tail) revealed that no difference exists in mean scarp height between the Dyer and Oasis sections at this level of significance. However, the midsection slope angles for these sections are different. All other results suggest different populations (separate fault sections).

If we assume a regular decrease in slope angle with estimated age for scarps of a given height, then the Oasis section in southern Fish Lake Valley appears to be the oldest. The wide range of scarp heights in the Dyer section, including the largest scarps examined in this study, suggests that this section has experienced repeated faulting over a long time period. Scarps measured as part of the Chiatovich Creek section are not as well correlated ( $R = 0.54$ ) as scarps found in the Dyer ( $R = 0.74$ ) and Oasis ( $R = 0.81$ ) sections. However, despite displaying more scatter, the regression line for the Chiatovich Creek section has a slightly greater (or steeper) slope. This would indicate that Chiatovich Creek, which is in the northern portion of Fish Lake Valley, may have the youngest scarps. The valley is also wider here than elsewhere. This greater width may be explained by the observation that the large, composite faults are generally confined within a 1 km zone along the FLVFZ, but here the surface rupture fans eastward away from the main fault into a "horsetail splay" (Sawyer, 1991).

The scarp morphometry from a series of profiles extracted from the DEM of Fish Lake Valley suggests that the oldest faulting occurred in the southern-most section (Oasis) and the most-recent faulting occurred in the northern-most section (Chiatovich). The middle section (Dyer) has the largest scarps. Furthermore, scarp morphometry, general terrain analysis using the DEM, and statistical analysis show that these subdivisions of previous workers are viable, perhaps only to be improved by better age control, which is currently unavailable.

## 6 CONCLUSIONS

The TOPSAR results presented here show the value of high-resolution digital topographic mapping for measuring morphometry of normal fault scarps

in relatively barren semi-arid regions, identifying fault scarps or fault-related lineaments, and quantifying slopes. There are small artifacts in TOPSAR elevations, as well as systematic differences between field measured and TOPSAR topographic profiles that point to the existence of potential problems in using TOPSAR data to interpret scarps less than  $\sim 10$  m in height.

Terrain analysis, scarp morphometry, and the statistical analysis of scarp components are consistent with previous field studies of scarp morphology. Scarp morphometry extracted from the Fish Lake Valley DEM suggests that the oldest faulting occurred in the southern-most section and the youngest faulting occurred in the northern-most section. The largest scarps are found in the middle section. Further studies of high-resolution DEMs can improve our understanding of the complexities of earthquake ruptures in complex tectonic settings.

### **6.0.1 Acknowledgments**

The TOPSAR data used in this study were analyzed and compiled by S. Hensley, S. Schaeffer, and E. Chapin at JPL. This work was supported in part by two generous grants from NASA.

## **References**

- [1] Brogan, G. E., Kellogg, K. S., Slemmons, D. B., and Terhune, C. L. (1991), Late Quaternary faulting along the Death Valley-Furnace Creek fault system, California and Nevada. U.S. Geol. Surv. Bull. 1991, 23 pp., scale 1:62,500.
- [2] Bucknam, R. C., and Anderson, R. E. (1979), Estimation of fault-scarp ages from a scarp-height-slope-angle relationship. *Geology* 7:11-14.
- [3] Crone, A. J., and Haller, K. M. (1991), Segmentation and the coseismic behavior of basin and Range normal faults: examples from east-central Idaho and southwestern Montana, U.S.A. *J. Struct. Geol.* 13:151-164.
- [4] dePolo, C. M., Peppin, W. A., and Johnson, P. A. (1993), Contemporary tectonics, seismicity, and potential earthquake sources in the White Mountains seismic gap, west-central Nevada and east-central California, USA. *Tectonophys.* 225:271-299.
- [5] dePolo, C. M., Clark, D. G., Slemmons, D. B., and Ramelli, A. R. (1991), Historical surface faulting in the Basin and range province, western North America: implication for fault segmentation. *J. Struct. Geol.* 13:123-136.
- [6] Gao, J. (1994), A C program for detecting slope forms from grid DEMs. *Earth Surf. Proc. Land.* 19:827-837.

- [7] Hensley, S., Rosen, P., and Zebker, H. (1994), Generation of high resolution topographic maps of the Galapagos Islands using TOPSAR data. International Geoscience and Remote Sensing Symposium, August 8-12, 1994, California Institute of Technology, Pasadena, Calif., pp. 704-706.
- [8] Madsen, S. N., Martin, J. M., and Zebker, H. A. (1995), Analysis and evaluation of the NASA/JPL TOPSAR across-track interferometric SAR system. *IEEE Trans. Geosci. Remote Sens.* 33:383-391.
- [9] Nash, D. B. (1980), Morphologic dating of degraded normal fault scarps. *J. Geol.* 88:353-360.
- [10] Nash, D. B. (1984), Morphologic dating of fluvial terrace scarps and fault scarps near West Yellowstone, Montana. *Geol. Soc. Amer. Bull.* 95:1413-1424.
- [11] Peterson, J. F. (1985), Equilibrium tendency in piedmont scarp denudation, Wasatch Front, Utah. In *Tectonic Geomorphology* (M. Morisawa and J. T. Hack, Ed.), (Proc. 15th Annual Binghamton Geomorphology Symposium), Allen & Unwin, Boston, pp. 209-233.
- [12] Reheis, M. C., and Dixon, T. H. (1996), Kinematics of the Eastern California shear zone: evidence for slip transfer from Owens and Saline Valley fault zones to Fish Lake Valley fault zone. *Geology* 24:339-342.
- [13] Reheis, M. C., and McKee, E. H. (1991), Late Cenozoic history of slip on the Fish Lake Valley fault zone, Nevada and California. In *Guidebook for field trip to Fish Lake Valley, California-Nevada* (M. C. Reheis, Ed.), Golden, Colo., Pacific Cell, Friends of the Pleistocene, pp. 26-45.
- [14] Reheis, M. C., and Sawyer, T. L. (1997), Late Cenozoic history and slip rates of the Fish Lake Valley, Emigrant Peak, and Deep springs fault zones, Nevada and California. *GSA Bull.* 109:280-299.
- [15] Reheis, M. C., Sawyer, T. L., Slate, J. L., and Gillespie, A. R. (1993), Geologic map of late Cenozoic deposits and faults in the southern part of the Davis Mountain 15' quadrangle, Esmeralda County, Nevada. *U.S. Geol. Surv. Misc. Invest. Series Map I-2342*, scale 1:24,000.
- [16] Sawyer, T. L. (1991), Late Pleistocene and Holocene paleoseismicity and slip rates of the northern Fish Lake Valley fault zone, Nevada and California. In *Guidebook for field trip to Fish Lake Valley, California-Nevada* (M. C. Reheis, Ed.), Golden, Colo., Pacific Cell, Friends of the Pleistocene, pp. 114-138.
- [17] Wallace, R. E. (1977), Profiles and ages of young fault scarps, north-central Nevada. *Geol. Soc. Amer. Bull.* 88:1267-1281.
- [18] Zebker, H. A., and Goldstein, R. (1986), Topographic mapping from interferometric SAR observations. *J. Geophys. Res.* 91:4993-4999.

- [19] Zebker, H. A., Werner, C. L., Rosen, P. A., and Hensley, S. (1994), Accuracy of topographic maps derived from ERS-1 interferometric radar. *IEEE Trans. Geosci. Remote Sens.* 32:823-836.
- [20] Zebker, H. A., Madsen, S. N., Martin, J., Wheeler, K. B., Miller, T., Lou, Y., Alberti, G., Vetrella, S., and Cucci, A. (1992), The TOPSAR interferometric radar topographic mapping instrument. *IEEE Trans. Geosci. Remote Sens.* 30:933-940.

## 7 TABLES AND FIGURES

Table 1: Morphometry derived from fault scarps in Fish Lake Valley

Site	Midslope angle ( $^{\circ}$ )	Scarp height (m)	Segment length (m)	n
Indian Creek	$23.0 \pm 3.8$	$34.3 \pm 5.4$	190	11
Indian Creek-South	$20.6 \pm 3.5$	$16.5 \pm 3.7$	180	19
Perry Aiken Creek-North	$23.5 \pm 3.9$	$43.3 \pm 8.7$	230	22
Perry Aiken Creek	$30.2 \pm 3.4$	$75.9 \pm 10.1$	290	30
Perry Aiken Creek-South	$22.8 \pm 3.8$	$37.2 \pm 5.5$	290	30
McAfee Creek	$24.2 \pm 4.2$	$38.4 \pm 6.7$	260	19
Wildhorse Creek	$17.6 \pm 2.8$	$45.9 \pm 11.6$	280	28

Explanation: measurements presented with standard deviation; n = number of measurements.

Table 2: Fault scarp morphometry for sections of the Fish Lake Valley Fault Zone

Section	Midslope angle ( $^{\circ}$ )	Scarp height (m)	n
Chiatovich Creek	$21.4 \pm 3.8$	$23.0 \pm 9.7$	30
Dyer	$25.4 \pm 4.9$	$50.2 \pm 18.6$	101
Oasis	$17.6 \pm 2.8$	$45.9 \pm 11.6$	28

Explanation: measurements presented with standard deviation; n = number of measurements.



Figure 1:  
Location map of Fish Lake Valley.

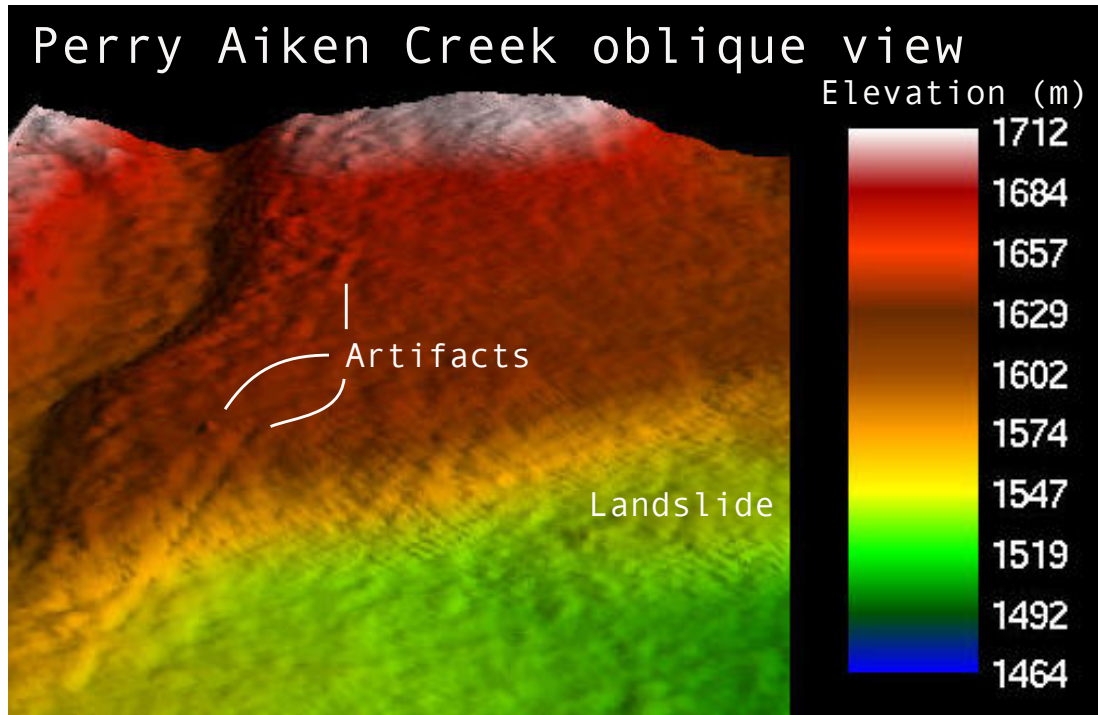


Figure 2:

Subset of the DEM around the 86 m-high fault scarp at Perry Aiken Creek. This oblique view looks west-northwest and is about 500 m across on the near side. A portion of the landslide deposit is also displayed. The low relief surface of the alluvial fan, interspersed with sagebrush community plants and boulders, displays a speckle or "pit-and-hummock" pattern that is inherent to radar data (e.g., Hensley et al., 1994). There is some "noise" in the data superimposed upon the relatively flat alluvial fan surface. These artifacts are labeled (arrows) and include an anomalous elevation value causing a small "cone" and a spurious line cutting across the southern margin of the large scarp. Visual ground inspection showed that these artifacts were not real.

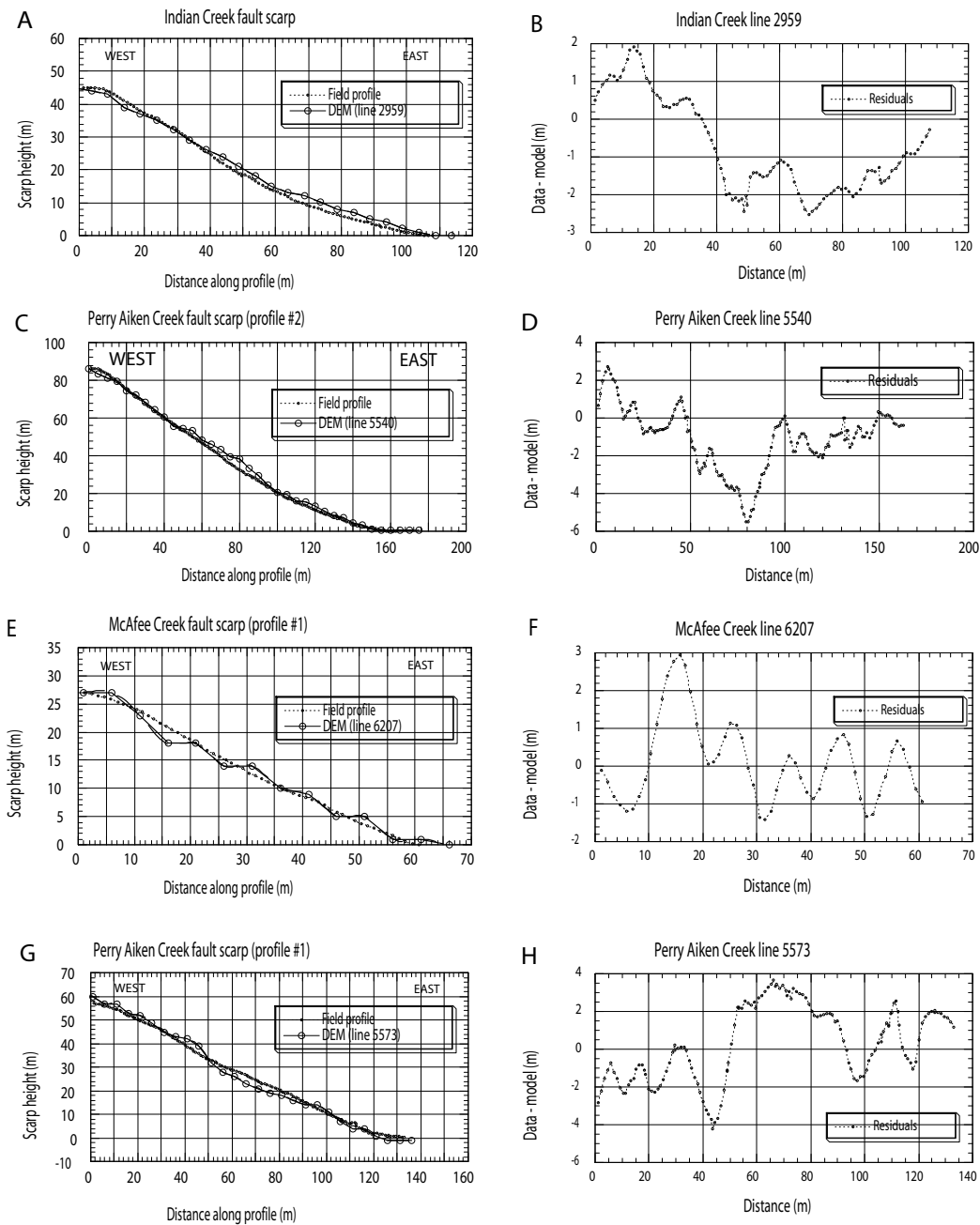


Figure 3:

Plots comparing ground truth (data) with the TOPSAR DEM (model) for profiles taken across scarp at four localities in Fish Lake Valley. Both ground-truth and TOPSAR DEM results are plotted on the left. Residuals for the same profiles are plotted on the right. Perry Aiken Creek-North is the only NW-SE trending scarp (others are about N-S); note its more convex profile.

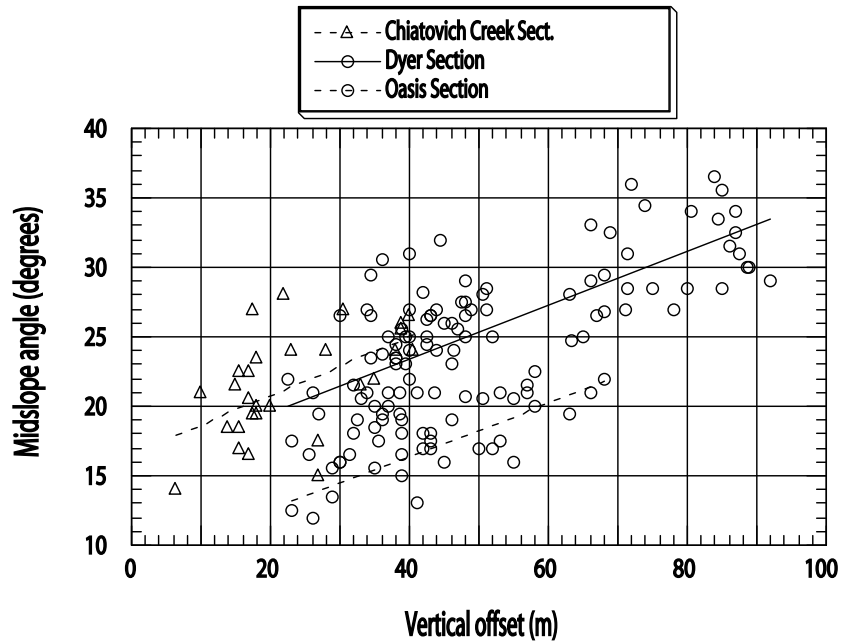


Figure 4:  
 Plot of scarp height versus midsection slope angle for each study site, arranged according to segmentation (Brogan et al., 1991; Reheis and Sawyer, 1997).